



ISTITUTO DI ANALISI DEI SISTEMI ED INFORMATICA
CONSIGLIO NAZIONALE DELLE RICERCHE

A. Bertuzzi, A. Gandolfi

**THE PROBLEM OF EVALUATING
THE IN VIVO CELL KINETICS IN TUMOURS**

R. 514 Novembre 1999

Alessandro Bertuzzi – Istituto di Analisi dei Sistemi ed Informatica del CNR, viale Manzoni
30 - 00185 Roma, Italy. Email : bertuzzi@iasi.rm.cnr.it.

Alberto Gandolfi – Istituto di Analisi dei Sistemi ed Informatica del CNR, viale Manzoni 30
- 00185 Roma, Italy. Email : gandolfi@iasi.rm.cnr.it.

This work was partially supported by the Progetto Strategico CNR “Metodi e Modelli Matematici nello
Studio dei Fenomeni Biologici”.

ISSN: 1128–3378

Collana dei Rapporti
dell'Istituto di Analisi dei Sistemi ed Informatica, CNR
viale Manzoni 30, 00185 ROMA, Italy

tel. ++39-06-77161

fax ++39-06-7716461

email: iasi@iasi.rm.cnr.it

URL: <http://www.iasi.rm.cnr.it>

Abstract

A survey of mathematical models used to estimate kinetic parameters of cell cycle or parameters related to the proliferation of a cell population using data of flow cytometry is presented in this work. Attention is focused on the analysis of sequential DNA-BrdUrd distributions that can be obtained from experimental tumours and on the estimation of T_S and T_{pot} from a single biopsy. The difficulties caused by the occurrence of cell loss are discussed and some models proposed to represent the proliferative heterogeneity of tumours are briefly presented. The assessment of the growth fraction of a cell population by proliferative markers and the methods for detecting the dead cells are finally considered.

Key words: Cell kinetics, tumour growth, DNA-BrdUrd flow cytometry.

1. Flow cytometry and in vivo cell kinetics

The first method that has been largely used to study cell proliferation in experimental and human tumours was based on ^3H -thymidine incorporation into S-phase cells. After ^3H -thymidine injection, DNA synthesizing cells incorporate the radioactive DNA precursor into the newly synthesized DNA and become thus labelled. The label is maintained upon cell division and is halved in daughter cells. Autoradiography of slices of the tumour sample taken some time after the injection allows to count the labelled cells and to determine the fraction of mitotic cells that are labelled. If a time sequence of samples following label injection is available, the time course of the labelling index (LI) and of the fraction of labelled mitoses (FLM) can be obtained. The FLM curve is related to the distribution of cell cycle phase transit times and thus to the distribution of the intermitotic time, and various mathematical models and computer programs have been proposed to extract the characteristics of the cell cycle from these curves [6,39,38,35]. Yet, when applied to the analysis of experimental data from tumours, these models often provided only a qualitative agreement with the behaviour of the curve after the first wave of labelled mitoses. Experimental data and curve analysis have been reported for various experimental tumours and for few *in vivo* human tumours. Ethical considerations prevented in fact the extensive use of radioactive thymidine administration with subsequent multiple biopsies in humans. A comprehensive account and a detailed discussion of these results can be found in Steel's book [37].

Autoradiography has the advantage of allowing the detection of morphologically distinct cells, but it is rather laborious and permits examining a small number of cells. This technique is currently replaced by flow cytometry. Flow cytometry (FCM) makes it possible to measure the DNA content and to detect other molecular constituents of the cell or probes, such as the halogenated analogues of thymidine, that can label the S-phase cells similarly to ^3H -thymidine. Thus, the most useful technique presently available for investigating the kinetics of cell populations is that based on the incorporation of the label bromodeoxyuridine (BrdUrd). In the following sections we describe and discuss mathematical models and methods that are useful for the *in vivo* estimation of kinetic parameters of tumours from flow cytometric measurements, and for the detection of markers related to cell proliferation and cell death.

2. The basic model

The usual approach to the quantitative analysis of flow cytometry data obtained from cell populations in unperturbed growth is based on a simple cell population model whose essential features can be found in Steel [37]. Although the basic assumptions of this model are rather restrictive for *in vivo* cell populations, the equations derived from this model are largely used. Let T_S and T_{G2M} denote the transit times in S and G2+M phases, respectively. We assume that: (i) the cell population is in asynchronous exponential growth (AEG), (ii) there is no cell-to-cell variability of T_S and T_{G2M} , (iii) no transition to quiescence occurs from S and G2M phases, (iv) cell loss affects all the cells of the population with a common rate constant (uniform cell loss). We observe that the time spent by a newborn cell to enter S phase is not required to be the same for all the cells of the population. Cells are allowed to decycle to a quiescent state Q after mitosis or from G1 phase, and cells from this resting state may reenter the cycle.

Equations for this basic model can be obtained as follows. Let us denote here as $n(a, t)$ the density with respect to age of cells in S+G2M phases, $n(a, t)da$ being the number of cells with age between a and $a+da$ at time t . Age a is counted from cell entry into S phase and

4.

$a \in [0, T_S + T_{G2M}]$. According to assumptions (ii), (iii) and (iv), $n(a, t)$ satisfies the continuity equation

$$\frac{\partial}{\partial t} n(a, t) + \frac{\partial}{\partial a} n(a, t) = -\mu n(a, t), \quad (1)$$

where μ is the rate constant of cell loss. In asynchronous exponential growth it is

$$n(a, t) = \bar{n} e^{-\beta a} e^{\alpha t} \quad (2)$$

with $\beta = \alpha + \mu$, α being the population growth rate constant, and the mitotic rate $g(t)$, *i.e.* the number of cells that undergo division in the unit time at time t , is given by

$$g(t) = n(T_S + T_{G2M}, t) = \bar{n} e^{-\beta(T_S + T_{G2M})} e^{\alpha t}. \quad (3)$$

We recall that $\alpha = \ln 2/T_d$, where T_d is the cell population doubling time. In the case of solid tumours, T_d can be identified with the volume doubling time, which is a measurable quantity. Under uniform random cell loss (assumption iv), the balance equation for the total number of cells, N , can be written as

$$\dot{N}(t) = g(t) - \mu N(t). \quad (4)$$

In exponential growth $N(t) = \bar{N} e^{\alpha t}$ and thus, from the above equation and Eq. (3), we have

$$\frac{\bar{n}}{\bar{N}} = \beta e^{\beta(T_S + T_{G2M})}. \quad (5)$$

By defining the rate constant of cell production, K_p , as

$$K_p = g(t)/N(t), \quad (6)$$

Eq. (4) gives $\alpha = K_p - \mu$ and then

$$\beta = K_p. \quad (7)$$

According to Steel, the potential doubling time of an exponentially growing cell population is defined as

$$T_{pot} = \ln 2/K_p \quad (8)$$

and thus, under uniform random cell loss, β can be expressed as $\ln 2/T_{pot}$.

To find the fraction of cells in S and G2M phases, f_S and f_{G2M} , the number of cells in S and in G2M is computed by integrating $n(a, t)$ with respect to age from 0 to T_S and from T_S to $T_S + T_{G2M}$, respectively. Taking into account (5), we obtain

$$f_S = e^{\beta(T_S + T_{G2M})} - e^{\beta T_{G2M}} \quad (9)$$

$$f_{G2M} = e^{\beta T_{G2M}} - 1. \quad (10)$$

Obviously, the fraction of cells in G1+Q is equal to $1 - f_S - f_{G2M}$. Therefore, from Eqs. (9) and (10), the ratios T_S/T_{pot} and T_{G2M}/T_{pot} can be easily expressed in terms of the fractions of cells in cycle phases:

$$\frac{T_{G2M}}{T_{pot}} = \frac{1}{\ln 2} \ln(1 + f_{G2M}) \quad (11)$$

$$\frac{T_S}{T_{pot}} = \frac{1}{\ln 2} \ln \frac{1 + f_S + f_{G2M}}{1 + f_{G2M}}. \quad (12)$$

The above equations are known as Steel's formulas. In the absence of cell loss we would have $\beta = \alpha$ and then T_{pot} would be equal to the population doubling time T_d . If even quiescent cells are not present in the population and all cells have the same cycle time T_c , T_d is equal to T_c . These conditions, however, do not occur in the *in vivo* tumour growth, so the T_{pot} in (11) and (12) is actually different from both T_d and T_c .

Regarding the technique of BrdUrd labelling, equations can be provided that relate the phase transit times to the evolution of the labelled subpopulations. The time course of the fractions of labelled cells after a BrdUrd pulse can be computed from the previous model (see [9]). In the case of *in vivo* labelling, when the label is delivered as a bolus or a short infusion, the duration of the time interval in which cells are exposed to BrdUrd is actually unknown, although it is thought to be short, so in most analyses the pulse is assumed of infinitesimal duration. Denoting by t the time elapsed after BrdUrd injection, the fraction of labelled undivided cells, $f^{lu}(t)$, can be written under the above assumptions as follows

$$f^{lu}(t) = \begin{cases} e^{\beta(T_S + T_{G2M} - t)} - e^{\beta(T_{G2M} - t)} & 0 \leq t \leq T_{G2M} \\ e^{\beta(T_S + T_{G2M} - t)} - 1 & T_{G2M} \leq t \leq T_S + T_{G2M} \end{cases} \quad (13)$$

From $t = T_{G2M}$ to $t = T_S + T_{G2M}$ the cells that undergo division are labelled, so a subpopulation of labelled divided cells arises. The fraction of labelled divided cells, $f^{ld}(t)$, can be obtained as

$$f^{ld}(t) = \begin{cases} 0 & 0 \leq t \leq T_{G2M} \\ 2[1 - e^{-\beta(t - T_{G2M})}] & T_{G2M} \leq t \leq T_S + T_{G2M} \end{cases} \quad (14)$$

Using $f^{lu}(t)$, the depletion function $DF(t) = \ln(1 + f^{lu}(t))$ [44] is obtained. The quantities f^{lu} and f^{ld} can be combined to give the so-called ν -function [47] defined as

$$\nu(t) = \ln \frac{1 + f^{lu}(t)}{1 - 0.5f^{ld}(t)}. \quad (15)$$

From Eqs. (13) and (14) it follows that, for $T_{G2M} \leq t \leq T_S + T_{G2M}$, $\nu(t)$ is constant and equal to

$$\nu(t) = \beta T_S. \quad (16)$$

The progression of the labelled cells across S phase can be quantitated by considering the time course of the mean red fluorescence (propidium iodide (PI) fluorescence) of the labelled undivided cells, F^{lu} . Begg *et al.* [7] defined the relative movement (of labelled undivided cells, RM) at time t as

$$RM(t) = \frac{F^{lu}(t) - F_{G1}}{F_{G2M} - F_{G1}} \quad (17)$$

where F_{G1} and F_{G2M} are the mean red fluorescences of G1+Q and G2M cells, respectively. An analytical expression of the relative movement has been obtained by White and Meistrich [46]. Under the hypothesis of linearity between DNA content and PI fluorescence, adding to assumptions (i)-(iv) the assumption of constant rate of DNA synthesis across S phase, it follows that:

$$RM(t) = \begin{cases} \frac{1 + \beta t - e^{-\beta(T_S - t)} - \beta T_S e^{-\beta T_S}}{\beta T_S (1 - e^{-\beta T_S})} & 0 \leq t \leq T_{G2M} \\ \frac{1 + \beta t - e^{-\beta(T_S - t)} - \beta T_S e^{-\beta(T_S + T_{G2M} - t)}}{\beta T_S (1 - e^{-\beta(T_S + T_{G2M} - t)})} & T_{G2M} \leq t \leq T_S \end{cases} \quad (18)$$

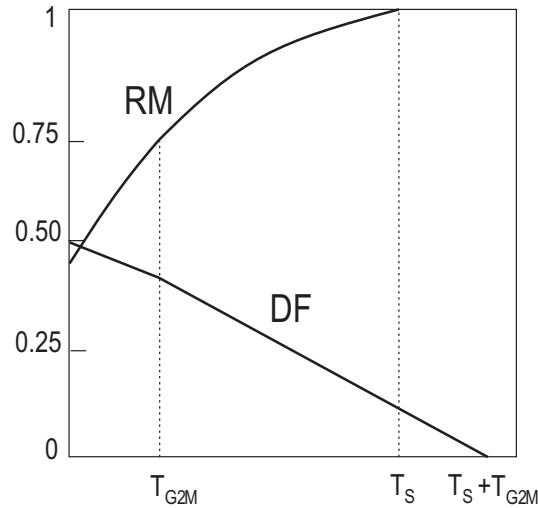


Fig. 1. Time courses of relative movement and depletion function of labelled undivided cells as predicted by the basic model.

The time course of DF and RM according to Eqs. (13) and (18) is shown in Fig. 1. Equations (13), (14) and (18) contain the kinetic parameters T_S , T_{G2M} and β , so these parameters, in principle, can be estimated by fitting f^{lu} (or DF), f^{ld} and RM data obtained from a time sequence of DNA-BrdUrd distributions. This application is possible in the study of experimental tumours implanted in animals [30]. Equation (18) was generalized to the case of non-constant rate of DNA synthesis across S phase [8].

3. Estimation of T_S and T_{pot} from a single delayed biopsy

Information on the kinetics of a human tumour can be obtained using only a single biopsy of the tumour, taken some hours (4-8 hours) following the BrdUrd administration [29,48]. From a single DNA-BrdUrd histogram, the relative movement at the time of biopsy can be determined and an estimate of T_S can be obtained. Begg *et al.* [7], approximating $RM(t)$ as a linearly increasing function with $RM(0) = 0.5$ (see Fig. 2), gave the following formula to estimate T_S from a DNA-BrdUrd histogram measured at time t after the BrdUrd injection:

$$\hat{T}_S = \frac{0.5 t}{RM(t) - 0.5}. \quad (19)$$

The Begg's formula is perhaps the most frequently used. An alternative formula, that has been derived from a different approximation of $RM(t)$ and requires an estimate of the fraction of cells in S and G2M, was given by White and Meistrich [46]. To estimate T_S when the labelling-biopsy interval is shorter than T_{G2M} , Ritter *et al.* [30] proposed to utilize the expression of $RM(t)$ given in [46] for a flat age distribution in S. A comparison among these equations when applied to simulated data can be found in [30].

Other formulas for the estimation of T_S were obtained by taking into consideration the fraction of labelled cells, instead of the relative movement. Durand [15] suggested to determine T_S assuming that the fraction of labelled cells in S phase decreases linearly with the time after labelling (this would actually occur if the cell age distribution in S were flat). A method that is still based on the labelled fractions, but uses a double labelling with two different halogenated

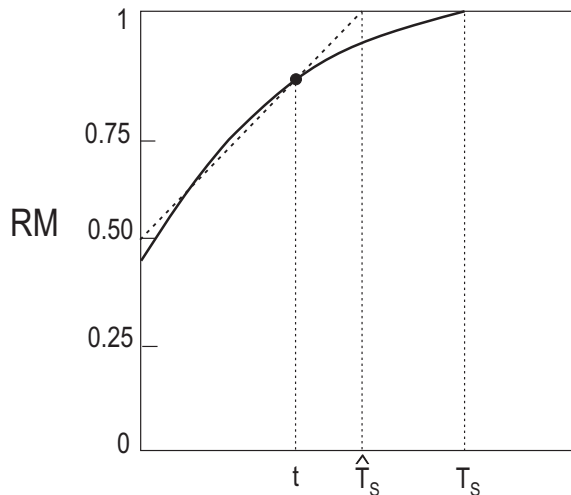


Fig. 2. Estimation of T_S from a single measurement of RM according to Begg's formula. The estimate is denoted as \hat{T}_S .

analogues of thymidine, was proposed by Ritter *et al.* [31]. After the injection of BrdUrd, a pulse of IdUrd (iododeoxyuridine) is delivered some hours later and thereafter the biopsy is performed. Two different monoclonal antibodies are used, one specific for BrdUrd and the other that recognizes both BrdUrd and IdUrd. From the two bivariate distributions of antibody content *vs.* DNA content thus obtained, it is possible to estimate both the fraction of cells that had been labelled with BrdUrd, denoted here as LI_{Br} , and the sum of the above fraction plus the fraction of cells that had been labelled only with IdUrd, $LI_{I/Br}$. When the cell age distribution in S is flat, assuming $LI_{Br} = f_S$, it follows that

$$LI_{I/Br} = LI_{Br} + LI_{Br} \Delta t / T_S \quad \Delta t < T_S \quad (20)$$

where Δt denotes the time interval between the pulses. An estimate of T_S is thus obtained from (20). The double labelling method was applied for studying experimental and clinical human tumors [31].

From a single histogram, after the estimation of T_S , also T_{pot} can be derived. Recalling that $\beta = K_p$, T_{pot} can be computed from (16) as

$$T_{pot} = \ln 2 \frac{T_S}{\nu}. \quad (21)$$

Another relationship that can be used to estimate T_{pot} was first derived by Steel (see [37]). From Eqs. (6) and (3), we have

$$K_p = \frac{n(T_S + T_{G2M}, t)}{N_S(t)} f_S \quad (22)$$

where $N_S(t)$ is the number of cells in S phase at time t . Computing $N_S(t)$ from Eq. (2), it is easy to see that the following equation holds

$$T_{pot} = \frac{\lambda T_S}{f_S} \quad (23)$$

with λ given by

$$\lambda = \frac{\ln 2}{\beta T_S} [e^{\beta(T_S + T_{G2M})} - e^{\beta T_{G2M}}]. \quad (24)$$

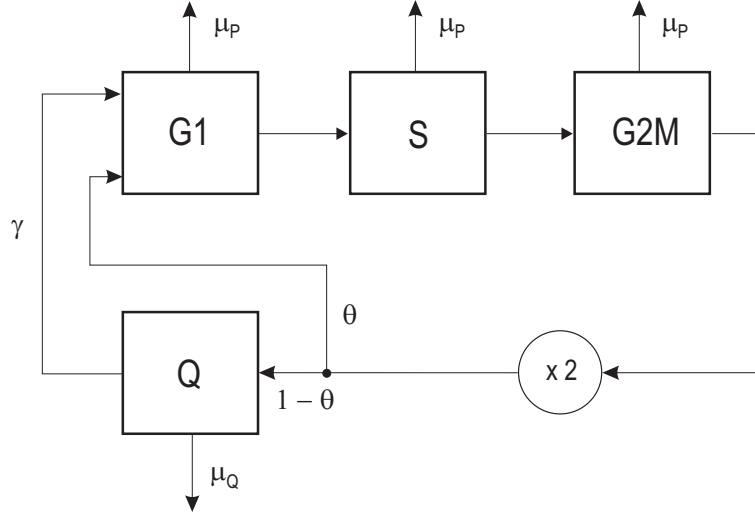


Fig. 3. Block diagram of the cell population model with reversible quiescence and nonuniform cell loss.

The quantities βT_S and βT_{G2M} take values from 0 to $\ln 2$ with the constraint $0 < \beta(T_S + T_{G2M}) < \ln 2$, so the theoretical range for λ is found to be $\ln 2 < \lambda < 2 \ln 2$. When both βT_S and βT_{G2M} tend to zero, λ tends to $\ln 2$. When T_S has been estimated, Eq. (23) becomes an operative formula if the coefficient λ is treated as an empirical parameter, usually set to 0.8 or 1. The fraction f_S , sometimes incorrectly identified with the labelling index LI at the measurement time t , can be more accurately estimated as

$$f_S = \frac{f^{lu}(t) + 0.5f^{ld}(t)}{1 - 0.5f^{ld}(t)}. \quad (25)$$

4. Growth fraction and nonuniform cell loss

In the tumour growth, a large fraction of cells appears to be nonproliferating and nonuniform cell loss is likely to occur. In particular, it is reasonable to assume that cycling and arrested cells are differently affected by cell death. Thus, to obtain kinetic information on tumours from cytometric measurements, the use of the model of section 2 could be inadequate. A compartment of quiescent cells can be considered separately from the compartment of G1 cells, and it can be assumed that newborn viable cells may enter G1 with probability θ or decycle to the quiescent state with probability $1 - \theta$. The possibility that quiescent cells reenter the cycle with a rate constant γ can be included. This model is depicted in Fig. 3.

The growth fraction of a cell population, GF , is defined as the ratio between the number of proliferating cells and the total number of viable cells. If we still assume that cell loss is uniform, under the simplifying hypothesis that all cells have the same cycle time T_c , a useful relationship among GF , T_{pot} , and T_c can be derived from the above model. Let $n_P(a, t)$ be the cell density with respect to age of proliferating cells. Age a is now counted from the start of G1 phase, so it is $a \in [0, T_c]$. In AEG we have $n_P(a, t) = \bar{n}_P e^{-\beta a} e^{\alpha t}$ and

$$g(t) = n_P(T_c, t) = \bar{n}_P e^{-\beta T_c} e^{\alpha t}. \quad (26)$$

From the balance equation (4), it is

$$\frac{\bar{n}_P}{N} = \beta e^{\beta T_c}. \quad (27)$$

Integrating $n_P(a, t)$ from zero to T_c to obtain the number of proliferating cells, and taking into account (27), we can write

$$GF = e^{\beta T_c} - 1. \quad (28)$$

Recalling that in the case of uniform cell loss it is $\beta = \ln 2 / T_{pot}$, we have the following relation [37]:

$$T_{pot} = \frac{\ln 2 T_c}{\ln(1 + GF)}. \quad (29)$$

If cell loss is not uniform, denoting by μ_P and μ_Q the rate constants of cell loss from the proliferative and the quiescent compartment respectively, the balance equation for the total number of cells can be written as

$$\dot{N}(t) = g(t) - \mu_P GF(t) N(t) - \mu_Q (1 - GF(t)) N(t). \quad (30)$$

From the above equation, dividing by $N(t)$ and assuming exponential growth, we obtain

$$K_p = \alpha + \mu_P GF + \mu_Q (1 - GF). \quad (31)$$

From Eq. (30), taking into account (26) and (31), we can also write

$$\frac{\bar{n}_P}{N} = K_p e^{\beta T_c}, \quad (32)$$

where now $\beta = \alpha + \mu_P$, so for the growth fraction we have

$$GF = \frac{K_p}{\beta} (e^{\beta T_c} - 1). \quad (33)$$

Although in the case of nonuniform cell loss K_p is different from β , as shown by Eq. (31), the relation (29) continues to hold approximately. When the argument of the exponential in (33) is small with respect to the unity, it is in fact $GF \simeq \ln 2 T_c / T_{pot}$. Thus, this approximation or Eq. (29) can be used in conditions of nonuniform cell loss to obtain an estimate of the cycle time T_c , provided that T_{pot} and an independent measurement of GF are available. We note that Eqs. (23) and (24) for T_{pot} still hold even if μ_Q is different from μ_P .

The occurrence of cell loss with different rates from the proliferating and the quiescent compartments affects both the relationships between phase fractions and relative durations of cell cycle phases and the time course of the fractions of labelled subpopulations after the BrdUrd pulse. The influence of nonuniform cell loss on the determination of the kinetic parameters of cell populations has been investigated in Bertuzzi *et al.* [9,10]. Here we illustrate how the Steel formulas (11) and (12) change. In exponential growth, expressing $g(t)$ in the balance equation (30) through Eq. (3) and taking into account (31), we have

$$\frac{\bar{n}}{N} = K_p e^{\beta(T_S + T_{G2M})}. \quad (34)$$

Thus, it is easy to obtain for the cell fractions in S and G2M the expressions

$$f_S = \frac{K_p}{\beta} [e^{\beta(T_S + T_{G2M})} - e^{\beta T_{G2M}}] \quad (35)$$

$$f_{G2M} = \frac{K_p}{\beta} [e^{\beta T_{G2M}} - 1], \quad (36)$$

from which the relations corresponding to (11) and (12) can be obtained. In the particular case in which cell loss is restricted to quiescent cells (*i.e.*, $\mu_P = 0$ and $\mu_Q > 0$), it is $\beta = \alpha = \ln 2/T_d$ and Eqs. (11) and (12) become:

$$\frac{T_{G2M}}{T_d} = \frac{1}{\ln 2} \ln(1 + \frac{T_{pot}}{T_d} f_{G2M}) \quad (37)$$

$$\frac{T_S}{T_d} = \frac{1}{\ln 2} [\ln(1 + \frac{T_{pot}}{T_d} (f_S + f_{G2M})) - \ln(1 + \frac{T_{pot}}{T_d} f_{G2M})]. \quad (38)$$

5. Proliferative heterogeneity

An essential aspect of cell proliferation in tumours is the heterogeneity of the population of proliferating cells, that exhibits a large variability of the cycle time and of the phase transit times. The variability of these kinetic parameters within the *in vivo* tumour cell population has been demonstrated since the early studies using ^3H -thymidine [37]. The proliferative heterogeneity can be related to the presence of subpopulations that are different on a genetic basis as well as to the different conditions of nutrition and oxygenation of the cells within the tumour.

In cell population models, the cell-to-cell variability of phase transit times has been considered both in the framework of branching process theory [43,21] and in the framework of the age formalism (for instance, see [12]). We report here the expressions for the asymptotic probability P_i that a cell randomly chosen from the population is in a given phase i (*i.e.*, the expected fraction of cells in phase i) in the simplified situation in which the transit times in the cell cycle phases are independent random variables, cell loss is absent, and all cells are cycling. Let $S_i = \sum_{j=1}^i T_j$, where T_i , $i = 1, \dots, 4$, are the times spent in G1, S, G2, and M phases respectively. It can be shown (see [43]) that the probability P_i is given by

$$P_i = 2\alpha \int_0^\infty [F_{S_{i-1}}(t) - F_{S_i}(t)] e^{-\alpha t} dt, \quad i = 2, 3, 4 \quad (39)$$

where F_{S_i} is the distribution function of S_i and α , given by

$$2 \int_0^\infty e^{-\alpha t} dF_{S_4}(t) = 1, \quad (40)$$

is the rate constant of the exponential growth that the expected total population size exhibits asymptotically.

Models and simulation programs developed to study the evolution of the labelled subpopulations after pulse labelling show, as expected, that if the transit times in S and G2M phases are distributed over the population, $RM(t)$ does not reach the unity for t equal to the mean value of T_S and $DF(t)$ remains larger than zero at the mean value of $T_S + T_{G2M}$. The behaviour of RM and DF in this condition has been investigated [46,44,4,42]. In [4], the relative movement measured in a human carcinoma transplanted in mice was more accurately fitted by assuming a large dispersion of S-phase duration, represented by a modified lognormal distribution. The occurrence of arrest of cell progression in G1, S, and G2M phases has been considered in a model

with no variability of phase durations, used for deriving expressions for $RM(t)$ and $DF(t)$ [45]. The major effect of the non-cycling S-phase cells on the relative movement is that the unity is not attained at any time and the depletion function does not vanish. These effects closely resemble those caused by the dispersion of transit times in S and G2M phases, making thus difficult to distinguish between these phenomena on the basis of the above kinetic data.

Simulation models with independently distributed cycle phase transit times and asymmetric transit-time distributions have been developed [51,41,5]. Baisch *et al.* [5] used the model to fit the fractions of cells in G1, S, and G2M of both labelled and unlabelled subpopulations after single or multiple labelling of an experimental tumour. The model included the possible transition to quiescence of cells from all cycle phases. The estimates obtained for the distribution of phase transit times showed a large dispersion, with a marked asymmetry towards the large values.

The aforementioned models, in the framework of age formalism, can be formulated as follows. Let $n_i^l(a_i, t)$ be the density of labelled cells in phase i with respect to the age a_i in that phase, i being equal to 1, 2, and 3 for G1, S, and G2M phases, respectively. Assuming that cells can arrest their progression across the cycle and so decycle to a quiescent state with rate constant ψ_i , and that only quiescent cells can be lost (as in [5]), we can write for the proliferating cells the following equations:

$$\frac{\partial}{\partial t} n_i^l(a_i, t) + \frac{\partial}{\partial a_i} n_i^l(a_i, t) = -[\beta_i(a_i) + \psi_i] n_i^l(a_i, t), \quad i = 1, 2, 3, \quad (41)$$

$$n_1^l(0, t) = 2 \int_0^\infty \beta_3(a) n_3^l(a, t) da \quad (42)$$

$$n_i^l(0, t) = \int_0^\infty \beta_{i-1}(a) n_{i-1}^l(a, t) da, \quad i = 2, 3, \quad (43)$$

where β_i is the age-dependent transition rate from phase i to phase $i+1$, β_3 being the mitotic rate. For the cells in the quiescent state we have:

$$\frac{d}{dt} Q_i^l(t) = \psi_i \int_0^\infty n_i^l(a, t) da - \mu_Q Q_i^l(t), \quad i = 1, 2, 3, \quad (44)$$

where $Q_i^l(t)$ is the number of labelled resting cells in phase i at time t and μ_Q the rate constant of cell loss. The transition rate $\beta_i(a_i)$ is related to the probability density function of the transit time in phase i in the absence of decycling, $p_i^0(a_i)$, by the equation

$$\beta_i(a_i) = \frac{p_i^0(a_i)}{1 - \int_0^{a_i} p_i^0(s) ds}. \quad (45)$$

In the case of pulse labelling at $t = 0$, the time course of the labelled subpopulations can be obtained from the previous equations with initial conditions:

$$n_1^l(a_1, 0) = 0, \quad n_2^l(a_2, 0) = n_2(a_2, 0), \quad n_3^l(a_3, 0) = 0, \quad (46)$$

$$Q_i^l(0) = 0, \quad i = 1, 2, 3, \quad (47)$$

where $n_2(a_2, 0)$ is the initial age density of cells in S phase. If the cell population is labelled in the condition of asynchronous exponential growth, the time course of the fractions of labelled

(and unlabelled) cells in the different phases can be computed after the AEG solution for the total population has been determined.

A different approach for representing the proliferative heterogeneity of tumour cell populations was proposed by Shackney [34] and recently reconsidered [36]. The cell population is assumed to be composed by m subpopulations characterized by different intrinsic cell cycle transit times T_{c_j} , $T_{c_j} < T_{c_{j+1}}$. At division, each cell of a subpopulation j generates cells initially belonging to the same subpopulation. As the cells of class j progress through the cycle, they can undergo a transition to the adjacent class $j+1$. This transition, denoted as growth retardation, allows the balanced exponential growth of the population to be maintained even in the presence of subpopulations with different and strictly inherited cycle times. From the biological viewpoint, the growth retardation in tumours can reflect the migration of cells from regions close to the vascular supply, that are characterized by fast proliferation, to regions with worse conditions of the microenvironment, characterized by slow proliferation and/or arrest of progression with subsequent cell death. We note that this model produces a certain degree of correlation among the durations of cell cycle phases, because a cell that has completed a phase in a long time enters the successive phase in a long cycle. This population model, complemented with a description of labelled thymidine incorporation after pulse or continuous labelling, was implemented as a computer simulation program and used for the analysis of FLM curves [35]. The model, after suitable modifications, could also be of interest for the analysis of time sequences of DNA-BrdUrd histograms from experimental tumours.

6. Measurement of growth fraction and detection of dead cells

The possibility of identifying the proliferating and the quiescent cells in a population is of primary interest, because the cells in a quiescent state have proved to be more resistant to anticancer therapies than proliferating cells. Thus, the assessment of the fraction of quiescent cells that retain the ability to re-enter the proliferative cycle may help planning the therapeutic regimens. Proliferating cells have recently been characterized by the presence of molecular markers, so these cells may be recognized by means of monoclonal antibodies and multiparameter flow cytometry or fluorescence microscopy of histological specimens (see the reviews by Danova *et al.* [13] and Yu *et al.* [52]).

Two nuclear antigens, PCNA and Ki-67, that are expressed in the proliferating cells and are absent or negligible in quiescent cells, and are thus believed to potentially provide an estimate of the growth fraction of a cell population, can be easily detected and quantitated. PCNA (Proliferating Cell Nuclear Antigen) is a protein involved in the process of DNA replication, that begins to be expressed in late G1, increases during S phase, and decreases at the transition from S to G2 and during G2M phase. Two forms of PCNA have been found: a bound (insoluble) form, detected as a “granular” staining from late G1 to G2M, and a second form which is detected as a diffuse staining throughout the whole cell cycle and is degraded with a long half-life of about 20 h. Because of this long half-life, PCNA is still present in quiescent cells, although at a low level. According to the experimental preparation method and to the anti-PCNA antibody used, the fraction of PCNA-positive cells may thus be related either to the S-phase fraction (similarly to the BrdUrd-positive fraction after pulse labelling) or to the fraction of proliferating cells in the population. See, however, the note of caution in [17] concerning the use of total PCNA immunostaining for the estimation of the growth fraction.

Particular attention is presently given to Ki-67, a nuclear antigen that appears to be involved in the process of condensation of chromosomes. The content and distribution of Ki-67 within

the cell nucleus changes during the cycle and its immunopositivity decreases rapidly near the end of mitosis. Because the expression of Ki-67 appears to be an essential requirement for cell proliferation [16], and since Ki-67 is absent in G0 due to its short half-life, this antigen is considered to be a good marker of proliferating cells. The so-called Ki-67 labelling index (or MIB-1 LI according to the anti-Ki-67 antibody used) is measured in human tumour samples also with the aim of assessing its prognostic value (see, for instance, [22] for breast cancer), and has been correlated to the measured T_{pot} in patients with head and neck cancer [50]. Other studies have shown the usefulness of the bivariate flow cytometry of PCNA *vs.* Ki-67 for recognizing the quiescent cells as Ki-67 (and PCNA) negative cells [25].

In contrast with the above described methods, in which the compartment of quiescent cells is recognized by the lack of certain proliferation-associated antigens, the expression of the nuclear protein statin appears to be a feature of quiescent cells both in culture and in the normal and tumour cells *in vivo*. It has been shown, indeed, that the fraction of statin-positive cells is inversely correlated with PCNA, Ki-67, and BrdUrd labelling indices [27] and that low fractions of statin-positive cells characterize highly malignant human tumours (see, for instance, [40] and [26]). When both Ki-67 and statin are detected, the Ki-67 negative fraction is generally larger than the fraction of cells expressing statin [27]. Thus, statin seems to mark the cells in a quiescence status deeper than that of simply arrested cells.

Other molecules that characterize the proliferative status of the cell are the cyclins, that are important components of the biochemical machinery which regulates the progression of cells through the cycle. For instance, cyclin E is a G1-cyclin with maximal expression at the G1/S boundary, and cyclin B1 is a G2-cyclin that controls the entry of cells into mitosis and is abruptly degraded at the end of this phase. Using monoclonal antibodies against the cyclins, it is possible to measure by bivariate DNA–cyclin flow cytometry the cyclin expression along the cell cycle [18,23]. An important point is also that the timing of cyclin expression may be markedly altered in tumour cell lines [18]: thus, the measurement of the expression of cyclins in the various cell cycle phases may provide new parameters of clinical interest.

A main factor that affects the growth of a tumour is the rate of cell loss. Cell loss from tumours mainly occurs because of physical detachment of cells from the tumour, due to exfoliation and metastasis, and because of cell death. Two distinct modalities of cell death, necrosis and apoptosis, are observed. Necrosis is a nonspecific mode of cell death caused by high concentration of toxic agents and hypoxia. Necrotic cells do not show immediate loss of DNA integrity, whereas the membrane integrity is rapidly lost. Apoptosis is a completely different phenomenon that is determined by “programmed” biochemical events, during which the cell membrane is preserved, DNA is cleaved into mono or oligonucleosome fragments and, successively, the cell separates into small apoptotic bodies.

Necrotic cells can be detected by flow cytometry because they have different scatter properties from viable cells. During the initial cell swelling, both forward and side scatter increase. In a later stage of necrosis, when there is loss of cell constituents because cell membrane is no longer intact, the scatter has a lower intensity. These differences, however, may be not sufficient to accurately discriminate dead cells from viable cells. Several dyes can be used to identify dead cells, since they are excluded from the viable cells as a result of high molecular weight or of the hydrophobic character of the molecule. Propidium iodide is excluded from entering the cell by an intact plasma membrane, but it can enter dead cells and bind to cell DNA. Because PI fluoresces only when it is bound to DNA, if the cells are incubated with PI only the nonviable cells will emit fluorescence. Propidium iodide has been largely used to exclude the dead cells in preparations examined for surface marker staining.

The discrimination among viable, necrotic, early apoptotic, and late apoptotic cells can be achieved by using the dyes Hoechst 33342 and PI and bivariate flow cytometry [28]. A more recent method for detecting apoptotic cells is based on an early event that occurs in cells undergoing apoptosis: the plasma membrane phospholipid phosphatidylserine is translocated from the internal to the external side of the membrane. If cells are incubated with the protein Annexin V (that has high affinity for phosphatidylserine) labelled with FITC, the apoptotic cells are detected as Annexin V–FITC positive cells. Thus, the bivariate flow cytometry PI *vs.* Annexin V shows the cells undergoing apoptosis as PI negative and Annexin V positive, whereas the late apoptotic cells are positive with respect to both fluorescences. The fraction of apoptotic cells in the subpopulation of CD34 positive cells of peripheral blood has been determined by Annexin V binding and bivariate FCM [1]. A different method for identifying the apoptotic cells exploits the fact that, because of DNA fragmentation, exposed 3'-hydroxyl DNA ends are abundant in apoptotic cells and these cells are thus able to bind to the exposed ends, in the presence of a suitable enzyme, large amounts of dUTP (deoxyuridine-triphosphate) conjugated with FITC. The apoptotic cells are so detected as those with higher FITC fluorescence. Measurements on samples from leukemic patients and on biopsies of solid tumours have been reported [19,20]. Methods based on flow cytometry for the investigation of apoptosis have been reviewed by Darzynkiewicz *et al.* [14]. Figure 4 gives a summary of molecular markers and probes used to identify different subpopulations in a cell sample.

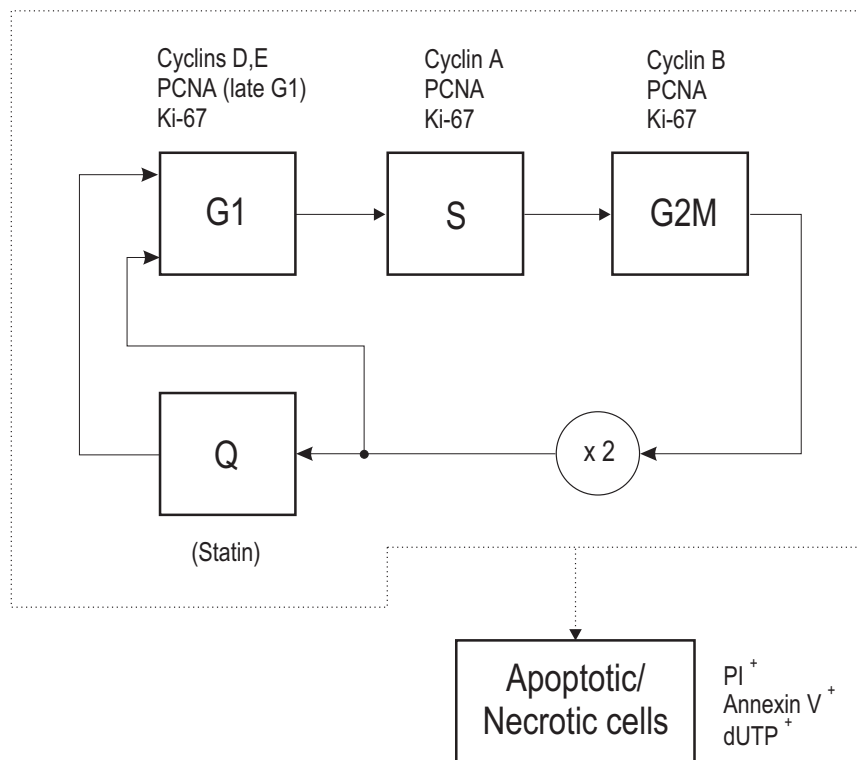


Fig. 3. Expression of markers of the proliferative or quiescent status and probes used to detect dead cells.

7. Comments

As a general comment to the previously discussed methods for the *in vivo* estimation of tumour kinetic parameters by flow cytometry, we note that difficulties in quantitative analysis can arise from the poor quality of FCM histograms, from cell heterogeneity of the bioptic sample, and from the presence of measurable dead cells.

As a consequence of the procedures used for obtaining a cell suspension from a solid tumour sample, the debris formed by fragmented cells or nuclei, and aggregates of cells and fragments, are present in large amount. The debris is well visible on the left of the G1 peak of DNA distribution, whereas the cell aggregates produce events that become visible on the right of G2M peak. The simplest way for taking into account cell debris in histogram analysis is to represent it by an empirical (exponential or power) function and to fit this function to the leftmost part of the histogram. The empirical distribution of debris is then subtracted from the measured histogram. A more sophisticated approach takes into account that the distribution of DNA content of debris is originated from the (unknown) distribution of DNA content in the cell population. The DNA distribution of debris thus also depends from the DNA distribution parameters of the cell population as well as from parameters related to the fragmentation process. A general expression of the fluorescence distribution of both cells and debris can then be obtained [32,2,11] and used for estimating all the parameters involved. Similarly, aggregates can be described using the probabilities of aggregate formation [3].

Because tumour cells are mixed with normal cells in the bioptic sample, when the tumour is aneuploid (that is, the DNA content of G1 tumour cells is different from the DNA content of G1/G0 normal cells) the fluorescence histogram of the sample shows multiple peaks. The DNA distribution analysis, in this case, should reconstruct the phase fractions of both tumour and normal cell populations and provide the DNA index (ratio of aneuploid to normal diploid DNA content). An algorithm for DNA distribution analysis of heterogeneous populations has been proposed [24]. From the DNA–BrdUrd distribution, it can be hard to determine the fractions of labelled tumour cells; in diploid tumours, in particular, the complete overlap of the tumour DNA distribution with the distribution of normal cells makes the analysis impossible if a specific marker of tumour cells is not available. For carcinoma cells, cytokeratin is a promising marker [33]. Other difficulties derive from the heterogeneity of proliferative characteristics in different regions of the tumour, as shown by the possibly large variability of potential doubling time and other parameters [49].

In the DNA–BrdUrd flow cytometry of a tumour sample, the population of measurable cells is larger than the viable tumour cell population because of the presence of normal cells and of tumour cells in early stages of necrosis. When apoptosis occurs, DNA is cleaved and DNA fragments are lost by the apoptotic cells, even in early-stage apoptosis, after the membrane permeabilization required for DNA staining. Thus, these poorly stained cells can be discriminated from viable cells [14]. On the contrary, DNA integrity is not immediately impaired in necrosis and the nuclei of early necrotic cells may also retain their integrity after the extraction procedure needed for flow cytometry of the suspension of nuclei, so these cells or nuclei cannot be distinguished from viable cells arrested in cycle progression. The influence of measurable dead cells on the fractions of labelled cells and on the estimation of T_{pot} has been investigated [9], and it has been found that this phenomenon can significantly affect T_{pot} estimation.

The above observations suggest therefore that a meaningful estimation of the kinetic parameters of a tumour requires carefully designed experimental planning, with multiple sampling of the tumour, the possible detection of suitable markers for tumour cells and for cell viability, and

the use of specifically designed software for histogram analysis.

References

1. R.S. Anthony, N.D. McKelvie, A.J. Cunningham, J.I. Craig, S.Y. Rogers and A.C. Parker (1998) Flow cytometry using annexin V can detect early apoptosis in peripheral blood stem cells harvests from patients with leukaemia and lymphoma. *Bone Marrow Transplant.* **21**, 441-446.
2. C.B. Bagwell, S.W. Mayo, S.D. Whetstone, S.A. Hitchcox, D.R. Baker, D.J. Herbert, D.L. Weaver, M.A. Jones and E.J. Lovett III (1991) DNA histogram debris theory and compensation. *Cytometry* **12**, 107-118.
3. C.B. Bagwell (1993) Theoretical aspects of flow cytometry data analysis. In *Clinical Flow Cytometry* (K.D. Bauer, R.E. Duque and T.V. Shankey, Eds.), Williams and Wilkins, Baltimore, pp. 41-61.
4. H. Baisch and U. Otto (1993) Intratumoral heterogeneity of S phase transition in solid tumours determined by bromodeoxyuridine labelling and flow cytometry. *Cell Prolif.* **26**, 439-448.
5. H. Baisch, U. Otto, U. Hatje and H. Fack (1995) Heterogeneous cell kinetics in tumors analyzed with a simulation model for bromodeoxyuridine single and multiple labeling. *Cytometry* **21**, 52-61.
6. J.C. Barrett (1966) A mathematical model of the mitotic cycle and its application to the interpretation of percentage labeled mitoses data. *J. Natl. Cancer Inst.* **37**, 443-450.
7. A.C. Begg, N.J. McNally, D.C. Shrieve and H. Kärcher (1985) A method to measure the duration of DNA synthesis and the potential doubling time from a single sample. *Cytometry* **6**, 620-626.
8. A. Bertuzzi, N. Del Grosso, A. Gandolfi, C. Sinisgalli and G. Starace (1995) Cell cycle analysis by the relative movement approach: effect of variability across S-phase of DNA synthesis rate. *Cell Prolif.* **28**, 107-120.
9. A. Bertuzzi, A. Gandolfi, D. Iacoviello and C. Sinisgalli (1997a) Steel's potential doubling time and its estimation in cell populations affected by non-uniform cell loss. *Math. Biosci.* **143**, 61-89.
10. A. Bertuzzi, A. Gandolfi, C. Sinisgalli, G. Starace and P. Ubezio (1997b) Cell loss and potential doubling times. *Cytometry* **29**, 34-40.
11. C. Bruni, L. Ferrante, G. Koch, C. Scoglio and G. Starace (1993) A stochastic model for cell debris in flow cytometry. *J. theor. Biol.* **161**, 157-174.
12. S.N. Chuang and H.H. Lloyd (1975) Mathematical analysis of cancer chemotherapy, *Bull. Math. Biol.* **37**, 147-160.
13. M. Danova, A. Riccardi and G. Mazzini (1990) Cell cycle-related proteins and flow cytometry, *Haematologica* **75**, 252-264.
14. Z. Darzynkiewicz, G. Juan, X. Li, W. Gorczyca, T. Murakami and F. Traganos (1997) Cytometry in cell necrobiology: Analysis of apoptosis and accidental cell death (necrosis), *Cytometry* **27**, 1-20.
15. R.E. Durand (1993) Determining T_{pot} in heterogeneous systems: a new approach illustrated with multicell spheroids. *Cytometry* **14**, 527-534.
16. M. Duchrow, J. Gerves and C. Schlüter (1994) The proliferation-associated Ki-67 protein; definition in molecular terms. *Cell Prolif.* **27**, 235-243.

17. P. Galand, G. Del Bino, M. Morret, P. Capel, C. Degraef, D. Fokan and W. Feremans (1995) PCNA immunopositivity index as a substitute to ^3H -thymidine pulse labeling index (TLI) in methanol fixed human lymphocytes. *Leukemia* **9**, 1075-1084.
18. J. Gong, X. Li, F. Traganos and Z. Darzynkiewicz (1994) Expression of G_1 and G_2 cyclins measured in individual cells by multiparameter flow cytometry: a new tool in the analysis of the cell cycle. *Cell Prolif.* **27**, 357-371.
19. W. Gorczyca, K. Bigman, A. Mittelman, T. Ahmed, J. Gong, M.R. Melamed and Z. Darzynkiewicz (1993) Induction of DNA strand breaks associated with apoptosis during treatment of leukemias. *Leukemia* **7**, 659-670.
20. W. Gorczyca, T. Tuziak, A. Kram, M.R. Melamed and Z. Darzynkiewicz (1994) Detection of apoptosis-associated DNA strand breaks in fine-needle aspiration biopsies by in situ end labeling of fragmented DNA. *Cytometry* **15**, 169-175.
21. P. Jagers (1975) *Branching Processes with Biological Applications*, Chichester: Wiley.
22. R.L. Jansen, P.S. Hupperets, J.W. Arends, S.R. Joosten-Achjanie, A. Volovics, H.C. Schouten and H.F. Hillen (1998) MIB-1 labelling index is an independent prognostic marker in primary breast cancer. *Br. J. Cancer* **78**, 460-465.
23. G. Juan, X. Li and Z. Darzynkiewicz (1997) Correlation between DNA replication and expression of cyclins A and B1 in individual MOLT-4 cells. *Cancer Res.* **57**, 803-807.
24. F. Lampariello and G. Del Bino (1988) Automatic parameter estimation of flow cytometric DNA distributions in the study of tumor cell kinetics. In *Proc. 8th IFAC/IFORS Symposium on Identification and System Parameter Estimation*, Beijing, 1988 (Han-Fu Chen, Ed.), Pergamon Press, pp. 1767-1771.
25. G. Landberg, E.M. Tan and G. Roos (1990) Flow cytometric multiparameter analysis of proliferating cell nuclear antigen/cyclin and Ki-67 antigen: a new view of the cell cycle. *Exp. Cell Res.* **187**, 111-118.
26. S. Pandey, P.H. Gordon and E. Wang (1995) Expression of proliferation-specific genes in the mucosa adjacent to colon carcinoma. *Dis. Colon Rectum* **38**, 462-467.
27. C. Pellicciari, R. Mangiarotti, M.G. Bottone, M. Danova and E. Wang (1995) Identification of resting cells by dual-parameter flow cytometry of statin expression and DNA content. *Cytometry* **21**, 329-337.
28. A. Pollack and G. Ciancio (1991) Cell cycle phase-specific analysis of cell variability using Hoechst 33342 and propidium iodide after ethanol preservation. In *Flow Cytometry* (Z. Darzynkiewicz and H.A. Crissman, Eds.), Academic Press, San Diego, pp. 19-24.
29. A. Riccardi, M. Danova, G. Wilson, G. Ucci, P. Dörmer, G. Mazzini, S. Brugnattelli, M. Girino, N.J. McNally and E. Ascari (1988) Cell kinetics in human malignancies studied with in vivo administration of bromodeoxyuridine and flow cytometry. *Cancer Res.* **48**, 6238-6245.
30. M.A. Ritter, J.F. Fowler, K. Youngmi, M.J. Lindstrom and T.J. Kinsella (1992) Single biopsy, tumor kinetic analyses: a comparison of methods and an extension to shorter sampling intervals. *Int. J. Radiat. Oncol. Biol. Phys.* **23**, 811-820.
31. M.A. Ritter, J.F. Fowler, K. Youngmi, K.W. Gillchrist, L.W. Morissey and T.J. Kinsella (1994) Tumor cell kinetics using two labels and flow cytometry. *Cytometry* **16**, 49-58.
32. W. Schmidt (1983) The problem of cell debris in pulse-cytophotometry: a probability theoretic model. *J. theor. Biol.* **103**, 581-599.

33. B. Schutte, M.M.F.J. Tinnemans, G.F.P. Pijpers, M.-H.J.H. Lenders and F.C.S. Ramaekers (1995) Three parameter flow cytometric analysis for simultaneous detection of cytokeratin, proliferation associated antigens and DNA content. *Cytometry* **21**, 177-186.
34. S.E. Shackney (1973) A cytokinetic model for heterogeneous mammalian cell populations I. Cell growth and cell death. *J. theor. Biol.* **38**, 305-333.
35. S.E. Shackney (1974) A cytokinetic model for heterogeneous mammalian cell populations II. Tritiated thymidine studies: the per cent labeled mitosis (PLM) curve. *J. theor. Biol.* **44**, 49-90.
36. S.E. Shackney and T.V. Shankey (1999) Cell cycle models for molecular biology and molecular oncology: exploring new dimensions. *Cytometry* **35**, 97-116.
37. G.G. Steel (1977) *Growth Kinetics of Tumours: Cell Population Kinetics in Relation to the Growth and Treatment of Cancer*. Oxford: Clarendon Press, pp. 189-191.
38. G.G. Steel and S. Hanes (1971) The technique of labeled mitosis - Analysis by automatic curve-fitting. *Cell Tissue Kinet.* **4**, 93-105.
39. M. Takahashi (1968) Theoretical basis for cell cycle analysis II. Further studies of labelled mitosis wave method. *J. Theor. Biol.* **18**, 195-209.
40. A.M. Tsanaclis, S.S. Brem, S. Gately, H.M. Shipper and E. Wang (1991) Statin immunolocalization in human brain tumors. *Cancer* **68**, 786-792.
41. P. Ubezio (1990) Cell cycle simulation for flow cytometry. *Comp. Meth. Programs Biomed.* **31**, 255-266.
42. P. Ubezio (1993) Relationship between flow cytometric data and kinetic parameters. *Eur. J. Histochem.* **37**/Suppl. 4, 15-28.
43. H. Weiner (1966) On age dependent branching processes *J. Appl. Probability* **3**, 383,402.
44. R.A. White (1989) Computing multiple cell kinetic properties from a single time point. *J. theor. Biol.* **141**, 429-446.
45. R.A. White (1991) A theory for analysis of cell populations with non-cycling S phase cells. *J. theor. Biol.* **150**, 201-214.
46. R.A. White and M.L. Meistrich (1986) A comment on "A method to measure the duration of DNA synthesis and the potential doubling time from a single sample". *Cytometry* **7**, 486-490.
47. R.A. White, N.H.A. Terry, M.L. Meistrich and D.P. Calkins (1990) Improved method for computing potential doubling time from flow cytometric data. *Cytometry* **11**, 314-317.
48. G.D. Wilson, N.J. McNally, S. Dische, M.I. Saunders, C. Desrochers, A.A Lewis and M.H. Bennett (1988) Measurement of cell kinetics in human tumors in vivo using bromodeoxyuridine incorporation and flow cytometry. *Br. J. Cancer* **58**, 423-431.
49. M.S. Wilson, C.M.L. West, G.D. Wilson, S.A. Roberts, R.D. James and P.F. Schofield (1993) Intra-tumoral heterogeneity of tumour potential doubling times (T_{pot}) in colorectal cancer. *Br. J. Cancer* **68**, 501-506.
50. G.D. Wilson, M.I. Saunders, S. Dische, F.M. Daley, B.M. Robinson, C.A. Martindale, B. Joiner and P.I. Richman (1996) Direct comparison of bromodeoxyuridine and Ki-67 labelling indices of human tumours. *Cell Prolif.* **29**, 141-152.
51. M. Yanagisawa, F. Dolbeare, T. Todoroki and J.W. Gray (1985) Cell cycle analysis using numerical simulation of bivariate DNA/Bromodeoxyuridine distributions. *Cytometry* **6**, 550-562.
52. C.C.W. Yu, A.L. Woods and D.A. Levison (1992) The assessment of cellular proliferation by immunohistochemistry: a review of currently available methods and their applications. *Histochem. J.* **24**, 121-131.